Physics Modeling for Steady-State Experiments at Wendelstein 7-X

J. Geiger 1), C.D. Beidler 1), M. Drevlak 1), Y. Feng 1), P. Helander 1),
N.B. Marushchenko 1), H. Maaßberg 1), C. Nührenberg 1), Yu. Turkin 1), P. Xanthopoulos 1)

1) Max-Planck-Institut für Plasmaphysik, EURATOM Assoc., 17491 Greifswald, Germany

e-mail address of main author: joachim.geiger@ipp.mpg.de

Abstract. The optimized stellarator Wendelstein 7-X (W7-X) is being built in Greifswald, Germany, as a superconducting device to show the inherent steady-state capability of stellarators at reactor-relevant parameters. For this purpose W7-X is equipped with a 10MW cw-ECRH system at 140GHz and a High-Heat-Flux divertor will be installed later capable of withstanding 10MW/m^2 to control particle and energy exhaust in steady-state operation. Here, we present physics predictions based on 1D-transport modeling using a neoclassical and a simple anomalous transport model to study the accessibility of high-performance plasmas under steady-state conditions. We investigate the most promising configurations of W7-X, the standard (SC) and the high-mirror configuration (HM). The SC shows good confinement making ‹β›-values of about 4% accessible for the given heating power, however, bootstrap currents up to 100kA can develop. In this case either current- or ι-control is necessary or the pulses are restricted to times smaller than the L/R-time on which the net current develops as W7-X has no ohmic transformer. On the other hand, the HM shows a 30% lower confinement than the SC, but the bootstrap current minimization is most effective and the net current is small allowing for stable boundary configurations, thus being compatible with steady state island divertor operation. The importance of developing an anomalous transport model is seen by the appearance of ITG-turbulence in a scenario with significant Ti-gradients. Also, the accessibility of improved fast-particle confinement in different W7-X configurations is discussed as this requires sufficiently high ‹β› and is thus dependent on the confinement properties.

1. Introduction

The stellarator Wendelstein 7-X (W7-X), under construction in Greifswald, Germany, is based on an optimized magnetic configuration[1] to overcome deficiencies of classical stellarators which would otherwise place serious limitations on future reactors. These shortcomings of stellarators are treated by the optimization criteria applied in the development of the W7-X configuration. These criteria comprise a high equilibrium- and stability-β of 4-5%, good neoclassical confinement, small bootstrap current and good fast particle confinement. Good neoclassical confinement is needed in a reactor to reach temperatures of about 15keV for ignition as the neoclassical electron heat conductivity grows in the most unfavorable case with $T^{7/2}$. The ‹β›-values are not only required to operate at moderate field strength to ease engineering requirements, but are also needed to generate the confinement of deeply trapped α-particles. In drift-optimized configurations with an appropriate toroidal mirror field the diamagnetism of the plasma generates quasi-isodynamic properties in the configuration (average minimum-B). As neoclassical transport properties depend on the magnetic configuration, the effect of β on the configuration should be small which closes the loop by requiring a high equilibrium-β, i.e. reduced Pfirsch-Schlüter currents resulting in stiffer configurations, and clearly the envisaged β-values should be reached without being threatened by MHD-instabilities. Additionally, a small bootstrap current is required by the island divertor concept for controlled particle and energy exhaust in steady-state operation. Limited current drive to control the boundary rotational transform ι_b needed for a stable separatrix is thus only compatible with small values of the bootstrap current. The optimization procedure resulted in a set of coils creating magnetic configurations that reconcile these different requirements [1].
This paper investigates the possibilities and limitations of combining these different goals with the given heating power in experimental scenarios at full field – for W7-X about 2.5T.

2. W7-X

W7-X is a device with 5 field periods, an aspect ratio of 11 (R_{maj}=5.5m, a=0.5m) and a pentagonal appearance when viewed from above. The flux surfaces change from bean-shaped in the pentagon's corners(φ=0°), providing a strong average elongation, to a triangular shape in the half-period symmetry plane(φ=36°). The coil system consists of 5 non-planar coil types per half period (stellarator symmetry) forming the basic magnetic configuration. Each coil type can be supplied with an individual current to modify the form and strength of the toroidal mirror field thus influencing the number and location of trapped particles. There is an intrinsic mirror field in the so-called standard configuration (SC, ι_b=5/5) of mr=4.5% (mr=(B_{ax}(0°)-B_{ax}(36°))/(B_{ax}(0°)+B_{ax}(36°)), which can be varied to either increase mr, e.g. the high-mirror configuration (HM) with mr=10%, or to decrease mr, e.g. the low-mirror configuration (LM) with vanishing mr. Additionally, 2 planar coil types per half-period add flexibility allowing variation of the value of ι_b between 5/6 (so-called low-ι), and 5/4 (high-ι), and to control the horizontal shift of the magnetic axis.
W7-X is built with superconducting coils to demonstrate and exploit the inherent steady-state capability of stellarators, and is consequently heated by a powerful cw-ECRH-system [2] (10 gyrotrons at 140GHz, each with 1MW) located at the pentagon's corners, normally the high field location along the magnetic axis. To control the particle and power exhaust an island divertor is foreseen which makes use of the inherent island structures formed at the boundary in configurations with the major resonances connected with ι_b=5/6, 5/5 and 5/4. A High-Heat-Flux (HHF)-divertor will be installed later capable of withstanding heat loads up to 10MW/m^2 in steady state, but the initial operation of W7-X will first use an inertially cooled divertor of the same geometry allowing for up to 10s pulses at 10MW heating power.

3. Methods and Assumptions Used in Transport Modeling

The investigations of confinement and bootstrap current use a 1-D transport code [3] to solve particle and power balance equations complemented with diffusion equations for the radial electric field and the poloidal flux (equivalent to the current density evolution). The transport considered is derived from mono-energetic transport coefficients calculated with the DKES-code[4] based on free-boundary VMEC-calculations[5] to include β-effects. In order to explore the upper limit of the performance of W7-X, anomalous transport is only considered with a heuristic contribution proportional to 1/n in the outer part of the plasma and which smoothly decays to small values in the center to ensure the dominance of neoclassical transport. If a configurations fails in this best-case estimate due to large neoclassical transport, increased anomalous transport will only worsen the situation. For the simulations presented here, the particle density profile is held fixed (see Fig.1).

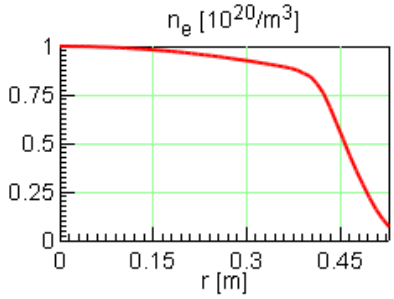

Fig. 1: Standard density profile form used in transport simulations.

4. Confinement

The effective helical ripple ε_{eff} is a figure of merit describing the neoclassical transport properties in the 1/ν-regime ($D_{11}^{1/\nu} \sim (\varepsilon_{eff})^{3/2} \cdot T^{7/2}/(n \cdot R^2 \cdot B^2)$, with temperature T, density n, major radius R and field strength B). As seen in Fig.2 showing ε_{eff} at half minor radius together with the trapped particle fraction, neoclassical transport is expected to be small for mirror ratios around 2-5% and increases for larger and smaller values of the mr. In configurations with neg-

ative mr the number of trapped particles is rather small but they are shifted to the location with strong radial drifts, i.e. the bean-shaped cross section. This strongly degrades the confinement. Fig.3 shows the ε_{eff}-profiles from the mirror-scan and for the reference low- and high-ι configuration with ι_b of 5/6 and 5/4, respectively, and a tendency for larger ε_{eff} values with increasing ι-values is found. On the other hand, there is a beneficial effect from increasing β. The Shafranov-shift leads to a decrease of the toroidal mirror field decreasing ε_{eff} as seen in Fig.3 (right) for the SC and HM.

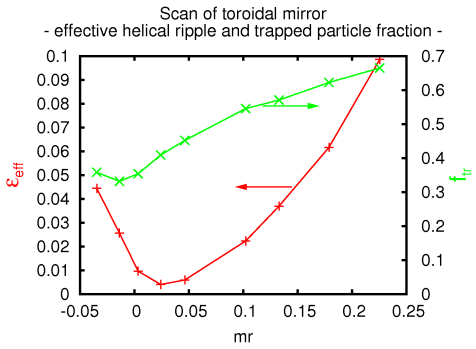

Fig. 2: Effective helical ripple and trapped particle fraction at half minor radius as a function of the mr for ι_b=1.

However, this only serves as a rough guide to the configuration dependence of neoclassical transport. In order to judge the performance of scenarios of primary interest, i.e. high-β in the long mean free path regime at full field strength, full transport simulations are needed due to the dependence on density, the strong non-linearity in T and the dependence of the transport coefficients on the ambipolar radial electric field as well as the electron-ion coupling.

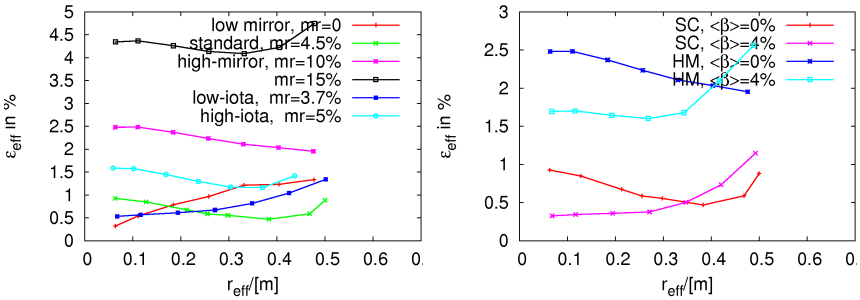

Fig. 3: Left: Effective helical ripple ε_{eff} for configurations varying the mirror ratio and ι. Right: Beneficial effect of β on ε_{eff}.

The first series of transport simulations considers a conservative heating scenario with 10MW ECRH X2-mode at a density of $10^{20}m^{-3}$ for on- and off-axis deposition. Fig. 4 (left) shows the plasma energies per volume to remove spurious size effects of different volumes of the equilibrium calculations reached in the three configurations LM, SC and HM scanning the mirror ratio from about 0 to 10% and including the effect of β (‹β›=0 and 4% for LM and HM, and 0, 2 and 4% for SC, denoted b0, b2 and b4 in the figure). The best confinement is seen in the SC with a weak dependence on the β-value. For HM there is an improvement with β as the mirror field is reduced, while the LM with 4% is degraded due to the inverted mirror field sign. The achieved ‹β›-values are in the range of 3.4% for the SC and about 3% for the HM. The difference between on- and off-axis deposition is only seen in the central electron temperatures (Fig.4 middle). On-axis deposition leads to the appearance of the electron root in the simulations and thus to higher central electron temperatures (see Fig.4, right). The appearance of a

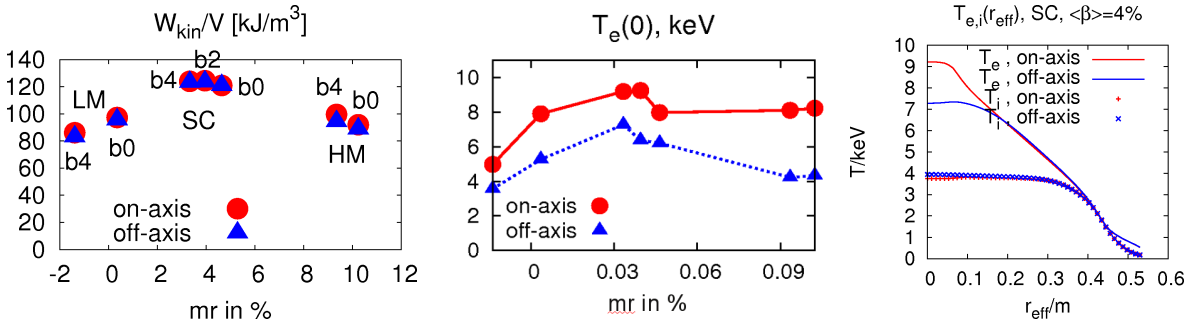

Fig. 4: Left: energy density for configurations with different mr-values. Middle: central temperatures achieved. Right: comparison of temperature profiles for on- and off-axis heating in SC with ‹β›=4%.

rather strong electron-root is the reason for the high central electron temperatures in the HM. Due to the small central volume the effect on the total confinement from this feature is negligible. Note, although there is a factor of about 4 difference between the values of ε_{eff} of SC and HM (see Fig.3) resulting in a factor of 8 ($(\varepsilon_{eff})^{3/2}$) in the 1/ν transport coefficient, the effect in the total energy is smaller, of the order of 25-30%. One reason is that the ions are less susceptible to neoclassical optimization and the strong coupling of electrons and ions in the outer part of the plasma leads to almost the same temperatures. The ions heat fluxes can thus dominate in the outer part and limit the total energy. Nevertheless, neoclassical optimization is necessary since to compensate a 30% degradation in confinement one would need an increase of the input power by a factor of 2 due to the power degradation of confinement (keeping all other parameters constant). Thus, to reach comparable energy values in the HM as in the SC would require about 20MW.

An alternative way to higher energy contents is suggested by the favorable dependence of the neoclassical confinement on density, which also agrees with scaling laws such as ISS04 [6]. Since higher densities lead to better electron-ion coupling, increasing the ion temperatures, this also leads to more reactor-relevant scenarios. However, higher densities require O2-heating with a cutoff density of $2.4\cdot10^{20}m^{-3}$ for a 140GHz ECRH system. Transport simulations assuming central electron densities of $1.8\cdot10^{20}m^{-3}$ with 10MW O2-heating lead to ‹β›-values around 4% for both SC and HM. Nevertheless, such a scenario is experimentally challenging as it requires a conventional start-up with X2 mode heating, followed by a controlled density ramp-up to around $10^{20}m^{-3}$ to make it possible to switch to O2-mode heating by changing the polarization, before increasing the density further.

The results so far suggest that with the assumption of neoclassical transport, ‹β›-values in the range of 3-4% may be achievable with 10MW ECRH-power. However, this relies on an optimistic model for the anomalous transport which is relevant only in the outer part of the plasma (r/a > 0.8). It is based on results derived from W7-AS, where high-performance discharges could be explained by neoclassical theory for r/a<⅔ [7]. As the neoclassical heat conductivity increases much more strongly with temperature ($\sim T^{7/2}$) than anomalous transport models usually do, this approach routinely leads to experimentally relevant values of $\chi_i > 1m^2/s$. The results may nevertheless be viewed as a best-case scenario, since turbulence is at present not included in the transport model. To fortify this expectation, a study of ITG turbulence [8] (adiabatic electrons, collisionless) is carried out with the GENE-code[9] extended over the entire plasma region. The analysis is based on a transport simulation with 6.5MW NBI ($P_{abs}\approx5.6$MW absorbed power) at $n_{e,0}=7\cdot10^{19}m^{-3}$ in the high-mirror configuration at 2.5T. This heating scenario was selected to generate strong ion temperature gradients over most of the plasma column. The GENE simu-

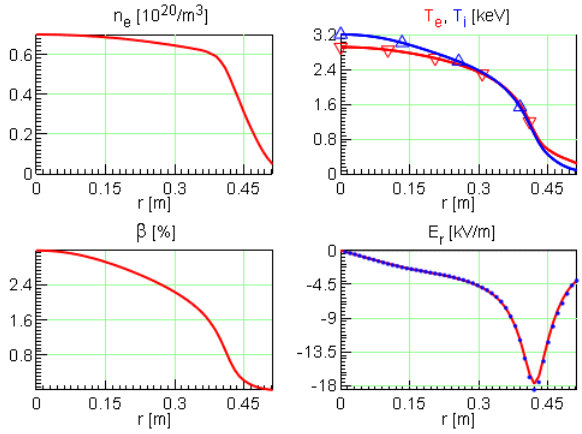

Fig. 5: Profiles resulting from transport calculations used to perform ITG-simulations with the GENE-code.

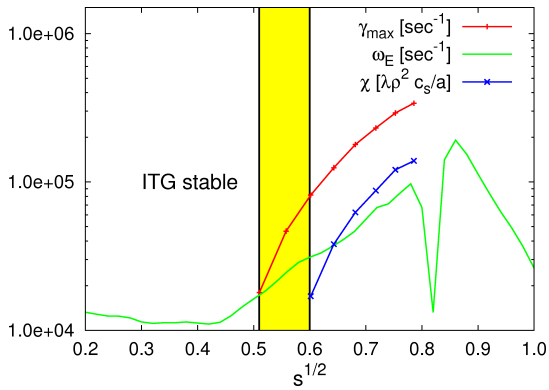

Fig. 6: Linear growth rate of ITG-modes and turbulent diffusivity from GENE-simulations and shearing rate of ambipolar radial electric field.

lations show that the ITG mode is unstable in the region beyond 60% of the minor radius (r>30cm), where the neoclassical transport coefficients fall rapidly due to their temperature dependence. In Fig.6, the turbulent ITG diffusivity is displayed rescaled in arbitrary units, to solely demonstrate its scaling. The absolute level is large enough to be of concern and will be needed when employing an anomalous transport model in the transport code (e.g. see [10]). Another significant component is the shear in the ambipolar radial electric field, which has not been included so far. Apparently, its magnitude would not fully suppress the ITG mode (gyrokinetic studies on MAST revealed that the shearing rate should exceed the growth rate of the fastest growing mode by 4-10 times), however it would certainly affect the calculated growth rates. A plausible next step towards such modeling is to calculate the critical gradients and derive a scaling of the turbulent diffusivity to incorporate into the transport code.

5. Bootstrap current

While neoclassical transport is governed by the radial drift of all trapped particles, the bootstrap current is mainly determined by the characteristics of the phase space boundary between trapped and passing particles. The minimization concept applied in W7-X balances the toroidicity driven part of the bootstrap current (ι-increasing) and the helically driven part (ι-decreasing). This is different from recent approaches in stellarator optimization studies trying to realize quasi-isodynamic configurations with poloidally closed contours of B. In such configurations both above mentioned parts of the bootstrap current vanish [11].

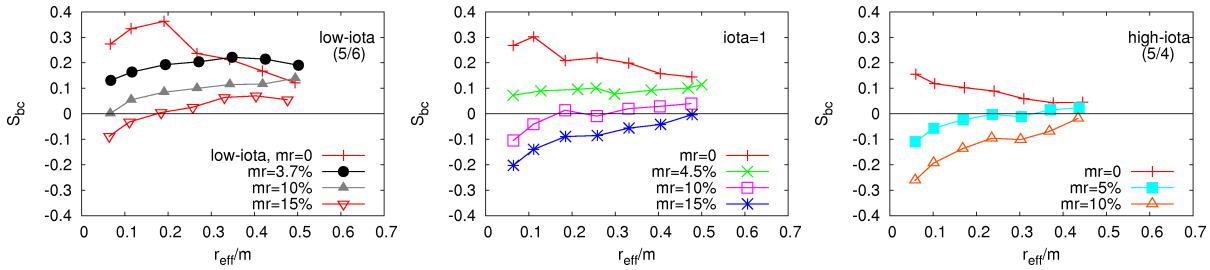

Fig. 7: Figure of merit S_{bc} for bootstrap current. mr-dependence for low- ι (left), ι=1 (middle) and high- ι (right). Values for vacuum configurations are shown.

In order to get an overview on the strength of the bootstrap current in different W7-X configurations, a new figure of merit, S_{bc}, is considered which is the (logarithmic) average of the bootstrap current coefficients for E_r=0 with respect to the collisionality normalized to the equivalent tokamak coefficients. This value reflects qualitatively sign and relative strength of the expected bootstrap current. Fig.7 shows the dependence with respect to the mirror ratio and with respect to ι. Note that the mirror ratio necessary for the balance of the two parts changes with ι, mr=5% for high- ι, but mr≥15% is necessary for low-ι. Thus, small bootstrap current and low neoclassical transport may not be achievable at the same time in the low-ι case. It should be noted that β leads to a positive contribution to S_{bc}.

This qualitative picture needs elaboration as the magnitude of the expected bootstrap currents scales with the plasma performance. Fig.8 shows the bootstrap current calculated for the heating scenario with 10MW X2-mode at $n_{e,0}=10^{20}m^{-3}$. The largest values are achieved in the SC and the smallest in the HM. Note that although the values of the bootstrap current in the SC are large

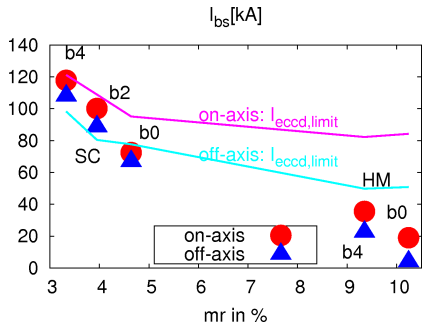

Fig. 8: Bootstrap current from transport simulation (10MW, X2-mode, on- and off-axis, $n_{e,0}=10^{20}m^{-3}$) for SC and HM. b0, b2 and b4 denote ‹β›=0, 2 and 4%. Solid lines indicate the limits for current drive with ECRH.

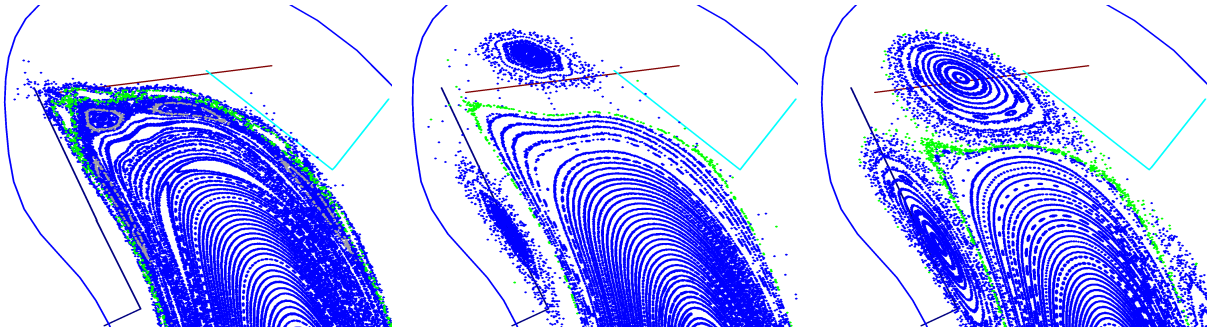

Fig. 9: Poincare plot showing the development to full toroidal current of a configuration adjusted for a bootstrap current of 43kA. From left to right: I_{tot}=0kA, 22kA, 43kA.

considering their impact on ι_b (10kA correspond to $\Delta\iota$=0.0176 at B=2.5T, R=5.5m and a=0.5m), they are still only about 10% of the value expected for an equivalent circular tokamak. Up to densities of $10^{20}m^{-3}$ ECRH with X2-mode provides sufficient current drive (see Fig.8), but for higher densities requiring the O2-heating scheme, current drive capabilities are insufficient. However, the magnitude of the bootstrap currents remain large in the SC. Depending on the considered β-configuration values between 40kA (‹β›=0) and about 80kA (‹β›=4%) are predicted. In the HM the bootstrap current reduces with higher density from ι-relevant values of a few tens of kAs (Fig.8) to values between -10kA to 10kA in O2-heating scenarios at $n_{e,0}=1.8\cdot10^{20}m^{-3}$. Together with the prior results on confinement, the HM seems feasible for a steady-state scenario with high-β at full field strength.

Considering the impact of net toroidal currents of more than 20kA ($\Delta\iota_b\geq0.035$) control of the value of ι_b is needed by either current drive or proper adjustment of the vacuum configuration. Further, considering the SC or any configuration with significant bootstrap current for use in an experimental scenario, the time-scales need to be considered on which the net toroidal current density evolves as W7-X has no ohmic-transformer. The fastest time scale is concerned with the particle and energy transport, characterized by the confinement time τ_E (on the order of a few hundred milliseconds). The next time scale is that on which the current density profile and thus the ι-profile evolves: the internal skin time (on the order of seconds) and finally, the global L/R-time (on the order of some tens of seconds), on which a non-zero net toroidal current grows.

The case of a freely evolving bootstrap current has been studied in a simulation for the SC at 2.5T with $n_{e,0}=1.5\cdot10^{20}m^{-3}$ with 7MW ECRH (140GHz, O2, on-axis). The final bootstrap current increases with an L/R-time of about 40s to about 43kA. The change of ι_b amounts to about 0.08 and would lead to a limiter-configuration if the vacuum configuration is not adjusted properly in advance. Such a scenario is rather challenging with respect to the evolution of the power load patterns on divertor tiles and other in-vessel components due to the long time scales. Fig.9 shows the configuration changes at time points t=0, 24s, +∞. Especially the slowly evolving strike line positions may be critical, e.g. in Fig.9 (middle) the separatrix crosses the pumping gap of the divertor. However, full 3D-edge transport simulations with codes like EMC3-EIRENE are needed to confirm the expectations numerically. Overloading of the HHF-divertor should be avoided as it will most probably cause serious damage.

The use of ECCD may lead to more feasible scenarios as the change of ι_b can be kept small in the time evolution. Fig.10 shows the evolution of the

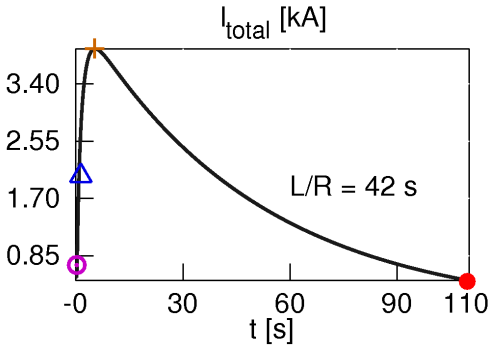

Fig. 10: Evolution of total current in case of off-axis ECCD compensating the bootstrap current.

total current of a transport simulation in the SC at 2.5T with $n_{e,0}=0.75\cdot10^{20}m^{-3}$ in which the ECRH power (140GHz, X2, off-axis) was switched from 1MW to 5MW. The launch angles of the ECRH beams were chosen such that the expected bootstrap current change would be compensated by the resulting ECCD [12]. Bootstrap current density and the current density of ECCD are driven at different radial locations and evolve on the internal skin-time which also differs radially. Thus a strong evolution of the ι-profile results which is depicted in Fig.11. Boundary-ι and the shear do not change significantly and a rather stable boundary structure is available for divertor operation. Nevertheless, the strong evolution of the current density and the ι-profile within the first seconds needs consideration. Local stability analysis [12] does not show instabilities for the simulated time points and the possible appearance of the natural 5/6-islands with an island width of 2.6cm at $r_{eff}\approx36$cm seems to be acceptable[13]. Using instead of off-axis ECCD the on-axis scenario because of its higher efficiency does not qualitatively change the picture. However, due to the strong central current drive the confinement in this region degrades as ι approaches values close to zero. This results in flat central temperature profiles and a broadening of the power and current deposition. This has been observed in high-power ECRH discharges with strong current drive at W7-AS [14]. These discharges were rather quiescent with no sign of MHD-instabilities.

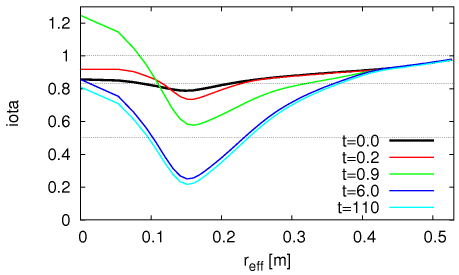

Fig. 11: Evolution of ι-profile in case of off-axis ECCD compensating the bootstrap current.

6. Fast particle confinement

The confinement of fast particles in W7-X relies on the diamagnetic effect to provide a uni-directional poloidal drift velocity for the fast particles trapped in a mirror field. This effect will appear in any configuration if ‹β› is large enough to create an average minimum-B configuration. In configurations with a toroidal mirror field this is more easily achieved. Fig.12 compares the collisionless loss rate of 60keV protons in the SC with good drift-optimization and a modified high-mirror configuration (MD) with mr≈10%. The particles are started at ¼ of the plasma radius, homogeneously distributed on the flux surface with random values of pitch angle. For a field strength of 2.5T the ratio of gyroradius to minor radius ρ_L/a for 60keV protons is roughly equal to that of 3.5MeV α-particles at 5T in a stellarator reactor. Both vacuum configurations do not confine the fast particles well and the initial losses consist of trapped particles leaving the plasma with the maximum drift velocity (for 60keV about 5km/s in W7-X). The β-values considered are not sufficient to completely suppress the losses in either configuration. However, while in the SC after an initial improvement stochastic collisionless losses are present, the MD confines the less deeply trapped particles increasingly better with higher ‹β›. An experimental investigation of this finite-β improvement would be based on the diagnostic beam used for CXRS using 60keV protons. The trapped particles generated in this way are not so deeply trapped as to be in the phase space region of the initial losses. Therefore, the improvement might be observable by the absence of fast particle losses for higher values of ‹β› in high-mirror configurations. The challenge in the experiments will be to get to the relevant ‹β›-values at densities which allow the diagnostic

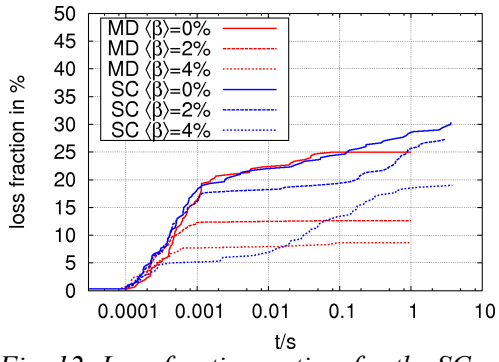

Fig. 12: Loss fraction vs time for the SC and a modified high-mirror configuration (MD) with mr=10%.

beam to penetrate deeply enough into the plasma. At this point the value of ε_{eff} of the HM is again of concern, prompting a search for configurations with good neoclassical confinement and better fast-particle confinement than offered by the high-mirror reference configuration using the flexibility of the W7-X coil system.

7. Summary and Discussion

Transport simulations for W7-X show that combining good neoclassical confinement with a small bootstrap current and good fast-particle confinement requires some care. In configurations with the lowest neoclassical losses, the bootstrap current tends to be of concern for the island divertor concept, which limits the net toroidal current to stay below 10kA due to its impact on the boundary island structure. ECCD can be used to "zero out" larger bootstrap currents in scenarios with densities up to $10^{20}m^{-3}$, where the X2-mode provides sufficient current drive capability. However, the strong ι-evolution on the time-scale of the internal skin-time cannot be eliminated and will be experimentally challenging. For operation at higher densities with O2-mode heating, configurations must be chosen with sufficiently small bootstrap current, which is provided by high-mirror configurations at ι_b=1 or with smaller mr-values at higher ι_b. Accounting for the net toroidal current effect on ι_b by properly adjusting the vacuum field is theoretically simple but experimentally very challenging due to the long L/R time-scales on which the plasma and its boundary structures evolve and may lead to critical power loads on parts of the divertor. Thus, steady-state operation with a greater flexibility in the choice of the configuration seems possible at moderate densities using ECCD for bootstrap current compensation and at higher densities (O2-mode heating) only in configurations with smaller bootstrap current. A larger variety of configurations may be used to investigate the confinement of thermal plasmas and of fast particles. This may require operating at high density to achieve the necessary β-values on time-scales short compared to the L/R-time but may have the disadvantage of significant bootstrap current. The present assumptions in the transport modeling also need improvement since initial investigations show that ITG-turbulence must be considered in the steep temperature gradient region in the outer third of the plasma.

References

[1] G. Grieger et al., *Phys. Fluids B* **4**, 2081 (1992)
[2] V. Erckmann et al., *Fusion Sci. Technol.*, **52** (2), 291, (2007)
[3] Yu. Turkin, *Fusion Sci. Technol.*, **50** (3), 387, (2006)
[4] W. I. van Rij and S. P. Hirshman, *Phys. Fluids B* **1** (3), 563 (1989)
[5] S. P. Hirshman et al., *Comput. Phys. Comm*., **43**, 143 (1986)
[6] A. Dinklage et al., *Nucl. Fusion*, **47**, 1265, (2007)
[7] J. Baldzuhn et al., *Plasma Phys. Control. Fus.*, **40** (6), 967, (1998)
[8] P. Xanthopoulos et al., *Phys. Rev. Lett.*, **99**, 035002 (2007)
[9] F. Jenko et al., *Phys. Plasmas*, **7** (5), 1904 (2000)
[10] M. Kotschenreuther, W. Dorland, *Phys. Plasmas*, **2** (6), 2381 (1995)
[11] P. Helander, J. Nührenberg, *Plasma Phys. Control. Fus.*, **51** (5), 055004, (2009)
[12] J.Geiger et al., *Contrib. Plasma Phys.*, **50**, 770 (2010)
[13] C. Nührenberg et al., *Phys. Rev. Lett.* **102**, 235001 (2009)
[14] H.Maaßberg et al., *Plasma Phys. Control. Fus.*, **47** (8), 1137, (2005)